Change Detection in Land Surface Temperature and Cooling Efficiency of Green Space in Phase One of the Federal Capital City, Abuja, Nigeria

***Ishaya S., Ayodeji Babalola Adejinmi & Abbas G Idriss**

Department of Geography and Environmental Management, University of Abuja, P.M.B. 117, Abuja

***Corresponding Author**

DOI: https://dx.doi.org/10.47772/IJRISS.2024.8120049

Received: 15 November 2024; Accepted: 26 November 2024; Published: 30 December 2024

ABSTRACT

This study uses geospatial techniques to detect changes in land surface temperature and cooling efficiency of green space in Phase One of the Federal Capital City, Abuja, Nigeria. Administrative boundaries shape file of 2023, Landsat imageries 4TM, 7ETM, 8OLI and 9TIRS and Thermal Near-infrared (7ETM, 8OLI and 9TIRS) were acquired from USGS Earth Explorer. The analyses of imageries were done within the ArcGIS 10.8 environment. In 1992 and 2002 green spaces covered the largest land area followed by built-up areas. In 2012 and 2022 built-up areas claimed the largest coverage area. From 1992 to 2002, the built-up area experienced the most significant change, showing an increase of 2.85 km2. During the same period, there was a loss in green space amounting to -2.13 km^2, while the bare surface increased by 2.27 km^2, from 2002 and 2012, the bare surface exhibited the most substantial change, experiencing an increase of 8.97 km^2, while the built-up area also increased by 6.75 km^2. Conversely, there was a significant decrease in green spaces, amounting to -18.72 km^2 during the same period. From 2012 to 2022, the built-up area experienced the most substantial change, showing a 9.93 km^2 increase. In contrast, bare surfaces decreased by -8.43 km^2, and green spaces also decreased by -1.52 km^2. From 1992 to 2002, an area with excellent cooling efficiency increased by 5.7 km2, an area with good cooling efficiency increased by 1.81 km^2, and an area with normal cooling efficiency increased by an infinitesimal area of 0.37 km^2. There was a decrease in an area with a bad cooling efficiency of -1.97 km^2, area with a worse cooling efficiency was reduced by -5.91 km2. From 2002 to 2012, an area with excellent cooling efficiency decreased to -5.59km^2, an area with good cooling efficiency decreased to -0.85km^2, an area with normal cooling efficiency increased to an infinitesimal area of 0.82km^2 and there was an increase in area with bad cooling efficiency with 1.55km^2, an area with worse cooling efficiency increased with 4.07km^2. From 2012 to 2022, an area with excellent cooling efficiency decreased by -1.22 km2, an area with good cooling efficiency decreased by -1.03 km2, and an area with normal cooling efficiency increased with a minute area of 0.73 km2 (1.187%). There was also an increase in area with a bad cooling efficiency of 0.82 km2, and worse cooling efficiency increased with 0.7 km2.

Keywords: Change, Detection, Surface, Temperature, Cooling, Efficiency, Green Space

INTRODUCTION

Rapid urbanization has become a distinguishing feature of the twenty-first century, as cities around the world continue to expand at an unprecedented rate (Zhaowu *et al.*, 2018). Over 2.5 billion more people are predicted to live in urban areas by 2050, with up to 90% of this increase concentrated in Asia and Africa, especially in China, India, and Nigeria, where 35% of urban growth is anticipated to occur (Chen *et al.*, 2018). This global urbanization process has resulted in a slew of environmental issues, the most visible of which is the urban heat island (UHI) impact. Natural landscapes are replaced by impervious surfaces, urban areas experience elevated land surface temperatures (LST) compared to their rural surroundings (Wong et al., 2017).

Studies have identified factors that could contribute to or worsen the urban land surface temperature effect, including changes in surface cover, increased human emissions, and urban growth **(**Balzarini, Paoletti and Van

Dingenen, 2009). These are caused by heat radiated from households, commercial, and industrial processes as well as heat retention in built materials (Baro *et. al.,* 2014). The resultant effect is increased cooling demand for buildings which transfer excess heat and humidity to the outside air leading to both increased heat and increased perception of heat in urban areas thereby posing a substantial threat to the well-being of urban inhabitants (Arnberger, *et. al.,* 2012).

Urban sustainability has become more of a concern as urbanization grows globally. Understanding the variations in LST and the cooling efficiency of green spaces within rapidly urbanizing areas is paramount for both urban climatology and society at large. It is impossible to overstate the benefits of nature in cities, and this has only helped us to realize how important urban green spaces (UGS) are for improving the ecology and sustainability of cities (Ishaya, 2020). Urban green spaces have many vital ecosystem services such as air cleaning, noise reduction, and carbon sequestration. Amid these great benefits of urban green spaces, the cooling effects via shading and evapotranspiration can mitigate the urban heat island effect. A decrease in vegetation, more specifically the absence of urban green spaces (trees, grasses, and bushes), results in an urban region being significantly warmer than the nearby rural areas.

The primary drivers behind the formation of UHIs are the replacement of vegetated surfaces with impervious materials, the modification of land cover, and changing energy balance within urban environments (Lindsey *et al.,* 2017). These factors increase heat absorption and reduce evaporative cooling, resulting in elevated LSTs and a localized warming effect in urban areas. Heightened heat stress is becoming more commonplace worldwide as a result of urbanization and climate change, this has led to several environmental problems which include temperature increases, changed patterns of precipitation, and higher energy use for cooling (Caiyan, *et. al*., 2021)

Trees, parks, gardens, and other forms of green infrastructure can mitigate the impacts of UHIs by lowering air temperatures, reducing energy demands for cooling, improving air quality, and enhancing the overall livability of urban areas. The urban climate environment is improved by vegetation shade because it reduces direct sunlight radiation, reflects short-wave radiation, and lowers the temperature by absorbing ambient heat through leaf transpiration (Sadroddin *et. al.,* 2014). This reduction in temperature is crucial for creating more comfortable living conditions and mitigating the heat island effect that is often exacerbated by impervious surfaces in cities. However, the cooling efficiency of green spaces can vary depending on factors such as vegetation type, density, arrangement, and proximity to built environments (Olubukola *et al.,* 2023). Urban heat in cities can be successfully reduced by green space through evapotranspiration and shadowing. (Ishaya, 2020). Land surface temperature (LST), which could be obtained from remotely sensed thermal infrared images, exhibits a strong relationship with air temperature and has shown to be a crucial data source for the study of Park Cool Island.

Nigerian towns and cities have undergone significant growth, characterized by urbanization rates ranging from 5% to 10% annually (Wong et al., 2021). This rapid urbanization has contributed to climatic irregularities within urban areas. Additionally, the utilization of construction materials such as cement asbestos, zinc, and aluminium roofing sheets has led to the dispersion of net radioactivity across different land uses, causing shifts in surface radiation patterns (Ishaya, 2020). The insufficient planning of urban land in Nigeria, coupled with high-intensity land use, has exacerbated various urban challenges, including the land surface temperature effect (Yan, *et. al.,* 2021). The escalating urban heat in Nigerian cities poses a substantial health risk to the growing population, and the associated heat stress is anticipated to intensify with rising temperatures, as observed by Oke (2017).

Over the years, the Federal Capital City (FCC) of Abuja has undergone a substantial urban transformation in the last decade, experiencing a more than twofold increase in its population, reaching a staggering 1.5 million residents. This surge in growth has positioned Phase One of the FCC as one of the most densely populated areas within the city of Abuja (FCTA Population Commission, 2021). Serving as the administrative, political, and economic hub of the Federal Capital Territory (FCT) Abuja, the FCC continuously attracts individuals seeking improved opportunities, intensifying the pressure on its infrastructure and green spaces. This rapid urbanization has led to significant alterations in land cover and land use patterns generating impervious surfaces, such as concrete and asphalt giving rise to the changes in land surface temperature contributing to the

emergence of UHIs (Isioye and Ikwueze, 2020). Recognizing the urgency of addressing the UHI issue, the FCT Administration has implemented initiatives, such as urban forestry programs, aimed at augmenting green cover and enhancing the cooling effect of green spaces in various districts (Tan and Jim, 2013). It becomes important to comprehensively examine the cooling efficiency of urban green spaces in Phase One of FCC Abuja's urban microclimate over an extended period.

The Study Area

The Federal Capital City (FCC) is situated in the Northeastern part of the Federal Capital Territory (Mabogunje, 1976). This area is recognized as highly suitable for human habitation and settlement development within the FCT (Balogun, 2001). Phase One of the FCC falls within latitude 9°6'17.28" to 9°6'25.812" and longitude 7°29'37.752 to 7°32'2.688" with an area coverage 69.4km^2. Phase One is segmented into five (5) districts, including Asokoro, Central Area, Garki, Maitama, and Wuse (Hassan and Ishaya, 2008) (See Figure 1).

The warm tropical savanna climate in this region contributes to the observed climatic conditions in the study area. During the dry season, temperatures tend to reach 30.2°C due to less cloud but the wet season experiences slightly milder temperatures, with the annual mean hovering around 25.8°C due to cloud cover prevalence. Phase One of the FCC and its surroundings record the highest annual rainfall, approximately 1,631.7 mm in the whole of the FCT due to orographic influence with more concentration of rainfall just within a few months, mainly in July, August, and September (Isioye and, Ikwueze, 2020). The terrain of Phase One of the FCC is characterized by hills and dissected features, making it the highest point in the FCT, with peaks reaching 760 meters above sea level (Balogun, 2001). The geological composition consists of basement complex rocks. The geological composition of Abuja encompasses a spectrum of rock formations, notably granite and schist. Aso Rock's granite structure is emblematic of the region's geological intricacies (Hassan and Ishaya, 2010). The topographical characteristics of Abuja are defined by undulating hills and plateaus, with the iconic Aso Rock serving as a geological landmark (Adakayi and Ishaya, 2016). The study area is majorly drained by River Usuma and most of the original vegetation of the area has been replaced with artificial plants (Isioye and, Ikwueze, 2020).

The demographic fabric of the study area is marked by diversity, with a burgeoning population engaged in multifaceted economic pursuits. As the administrative nucleus of Nigeria, the city hosts government institutions, foreign embassies, and an expanding service sector, contributing significantly to its economic vibrancy and population diversity (Adakayi and Ishaya, 2016). In terms of infrastructure, the FCC boasts of a well-developed network of roads, electricity supply, drainage and sewage systems, and piped water.

Figure 1: Phases of the Federal Capital City's (FCC) Development

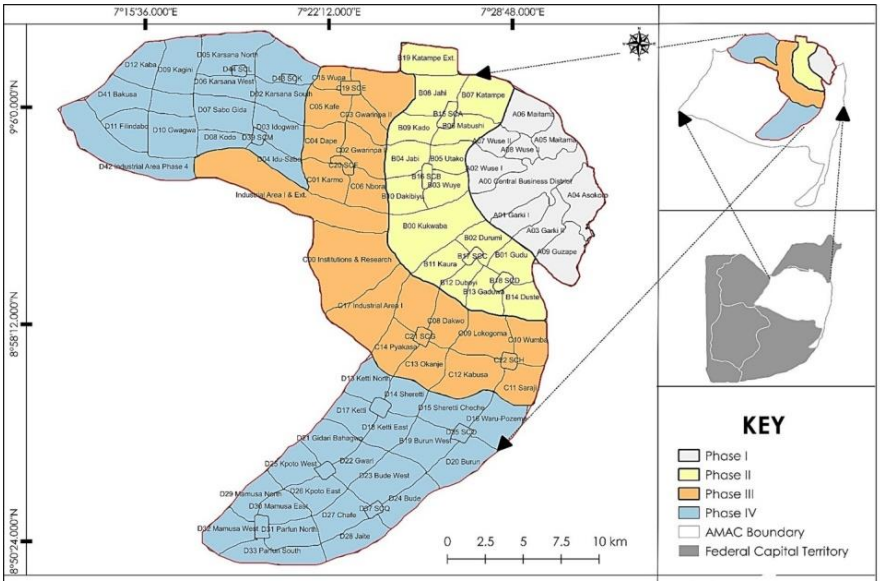

Source: Ezeamaka & Oluwole (2016)

ISSN No. 2454-6186 | DOI: 10.47772/IJRISS |Volume VIII Issue XII December 2024

METHODOLOGY

This research adopted a geospatial technique in assessing the land use land cover change dynamic, LST and cooling efficiency of the urban green using the ecological evaluation index from 1992-2022.

Types and sources of data used

Landsat imageries were acquired from USGS Earth Explorer by navigating to the area of interest using the pan tool and utilising the drag tool to delineate the area of interest. The images as well as the administrative boundary shape file of the study area were downloaded through the USGS global visualization viewer (Glovis). The administrative boundary was obtained from the Department of GIS and Cartography in the Office of Surveyor General of the Federation and the Landsat imageries were downloaded from an open source (See Table 1). Ground truth data were obtained for the land use of Phase One of the FCC Abuja using Garmin 60 Cx GPS to ascertain geographical locations of land use/land cover to train pixels during classification.

Table 1: Data Types and Sources

S/N	Data	Resolution	Year	Source	Relevance
1	Administrative boundaries shape file		2023	OSGOF	To define the spatial boundary
2	Landsat imageries 4TM, 7ETM, 8OLI and 9TIRS	30mx30m	1992,2002, 2012 and 2022	Earth explorer USGS	For land use land cover
3	Thermal Near-infrared (7ETM, 8OLI and 9TIRS)	30mx30m	1992,2002, 2012 and 2022	Earth explorer USGS	For land surface temperature and urban thermal fluid variance index

Source: Researcher Compilation, 2024.

Technique of data analysis

The downloaded images were extracted and then layer stacked using Arc GIS software 10.8 to give a false-colour composite image using bands like 4, 3, and 2. The layer-stacked images were then sub-set to the area of interest (FCC) for visualization and to enable proper analysis.

Identify and map LULC within Phase One of the FCC (1992-2022)

The administrative boundary shape file was obtained from the office of the survey general of the federation, it was projected and transformed from World Geodetic Coordinate 1984 to Universal Transverse Mercator zone 32N Minna. However, cartographic embellishment and annotation were done in ArcGIS 10.8.

Satellite/Digital image preprocessing

This preprocessing is intended to correct errors in the pixels. The images were processed both geometrically, radiometrically, and spatially filtered to suppress the errors arising from either the sensor, noise, sun angle or atmosphere effect. The essence of image enhancement in this study was to reduce the visual complexity of the images and also to improve the visual quality and recognition of features for easy image interpretation. Sub-setting which involved clipping in the area of interest on the composite layer using extract by mask module on ArcGIS software interface for further preprocessing steps was carried out before training sampling and creating a signature file that assigned the sample to the composite layer according to the feature spectral reflectance using training manager and creating the signature file as an extension file to enable the maximum likelihood classifier function.

ISSN No. 2454-6186 | DOI: 10.47772/IJRISS |Volume VIII Issue XII December 2024

Image Classification

Regarding this study, a supervised classification approach was adopted using an interactive maximum likelihood algorithm for the classification of the images. Considering the visual and digital interpretation of satellite images as well as the need for this study, three land use/land cover types were examined (built-up, Bare Surface and Green Space). The vectorization was done to convert the raster to a polygon for the calculation of geometry.

Performing a land cover change matrix detection from 1992 to 2022

The change detection method used in this study is the 'Area Analysis method'. This involves the analysis which highlights the trend and rate of different land use (LU) changes over the period under assessment. There are three (3) levels embarked on in computing the change detection for each LU by area statistics which involve;

i. The first stage involves the calculation of the magnitude of change and this is done by subtracting the observed change of each period of the year from earlier periods of the year.

ii. The next step is the calculation of the percentage change of each of the land use (trend), this was achieved by subtracting the percentage change of the previous land use from the recent land use, divided by the previous land use and multiplied by 100. Consequently, this will help assess at a glance, the spatial extent of LU gained or lost.

iii. Finally, the last step involves the calculation of the annual rate of change by dividing the percentage change by 100 and multiplying by the number of study years, which is 10 years.

Assessing the LST and decadal changes in Phase One of FCC from 1992 to 2022

Imported the multispectral thermal image (Band 6, 10) through Add data and catalogue Landsat 4_{TM}, 7_{ETM} spectral radiance data has also been converted to planetary TOA reflectance. Using coefficients of reflectance rescaling provided in metadata associated with the Landsat $7_{ETM.}$

For converting DN values into TOA reflection in the ETM image use the following equation:

$L_1 = (L_{max} – L_{min} / QCAL_{max} – QCAL_{min}) * (QCAL – QCAL_{min}) + L_{min}$……. Equation 1.

Where;

L = Spectral radiance.

QCAL = Quantized Calibrated Pixel Value in Digital Number.

L_{max} = Spectral radiance scaled to $QCAL_{max}$ in watts

L_{min} = Spectral radiance scaled to $QCAL_{min}$ in watts

$QCAL_{max}$ = Maximum quantized calibrated pixel value

$QCAL_{min}$ = Minimum quantized calibrated pixel value

Conversion radiance into Bright Temperature (In kelvin)

$$L = \frac{K2}{\frac{K1}{L}+1}$$ ……...Equation 2

Where;

ISSN No. 2454-6186 | DOI: 10.47772/IJRISS |Volume VIII Issue XII December 2024

K1 and K2 = specific thermal conversion constant from the Metadata (From obtaining the result in Celsius the radiant temperature is revised by adding the absolute zero (approx.-273.15).

Secondly, the reflectance value from the satellite data Landsat 8 $_{OLI}$ was calculated. Landsat 8 $_{OLI}$ spectral radiance data was also been converted to planetary TOA reflectance using coefficients of reflectance rescaling provided in the Landsat 8 $_{OLI}$ file. For converting DN values into TOA reflection in the OLI image use the following equation:

Formulae; L^ = ML * QCAL + AL – O_i……. Equation 3

Whereas

L^ = Atmosphere Sensor Temperature (AST)

ML = Radiance Multiplicative Band 10

AL = Add a band

QCAL = Quantized and calibrated standard produce pixel value band 10

0i = Correction value for band 10 = 0.29

Conversion AST to Bright Sensor Temperature

Formulae; Kelvin to Celsius

BT = K2/Ln (K1/L^+1) – 273.15 …….. Equation 4

Where;

K1 and K2 = Specific thermal conversion constant from the Metadata (From obtaining the result in Celsius the radiant temperature is revised by adding the absolute zero (approx.-273.15).

Normalized Difference Vegetation Index

NDVI is a standard vegetation index calculated using near-infrared and red.

Formulae;

Float (NIR – RED) / Float (NIR + RED) ……. Equation 5

Whereas

NIR = Band 5

RED = Band 4

Land surface emissivity.

Land surface emissivity is the average emissivity of an element on the surface of the earth calculated from NDVI

Formulae;

PV = square ((NDVI - NDVI min)/ (NDVI max – NDVI min)) ……. Equation 6

E = 0.004 * PV + O.986 ……. Equation 7

Whereas

NDVI max = High value

NDVI min = Low value

PV = Proportion of vegetation

0.986 corresponds to a correctional value of the equation.

Land surface temperature

The land surface temperature is the radioactive temperature calculated using an atmosphere sensor of temperature, brightness, wavelength of emitted radiance, and land surface emissivity.

Formulae;

LST = BT / (1+ (^*BT/C2) * Ln (E)) ……. Equation 8

Here, C2 = 14388µmk

The value of the ^ for Landsat 8 for band 10 is 10.8 and band 11 is 12.0

For which the peak response and the average of the limiting wavelength

(^ = 10.895), Source: (Wang *et al*, 2009)

Where;

BT = Bright Temperature

^ = Wavelength of the emitted radiance

E = Land surface emissivity

H = Planck‘s constant = 6.626 * 10-34

S = Boltzman constant = 1.38 * 10 -23

C = Velocity of light = 2.998 * 103

C2 = H * C/S

Evaluate the cooling efficiency of green spaces within the FCC from 1992 to 2022

The UTFVI was used in this study. The UTFVI measures urban ecological quality of life in terms of the degree of thermal comfort relative to the existence of the UHI phenomenon. Therefore, it was used to detect varying impacts of the urban heat in the study area. To illustrate the level of EEI impact more clearly, the result of UTFVI was categorized into six classes (Table 3.3) (Zhang, 2006), and each category corresponds to a fixed ecological evaluation index (EEI). UTFVI is frequently used to evaluate the impact of land surface temperature on ecosystem effect. It was calculated using the following model:

$$UTFVI = (T_S - T_{mean})/SD \quad \text{Equation (9)}$$

Where;

Ts is the LST at certain points of the map and Tmean is the corresponding mean temperature of the whole area.

Table 2: Threshold of ecologically evaluation index

S/N	UTFVI	EEI
1	< 0	Excellent
2	0.000–0.005	Good
3	0.005–0.010	Normal
4	0.010–0.015	Bad
5	0.015–0.020	Worse
6	> 0.020	Worst

Source: Zhang, (2006).

Figure 2: Study Methodology

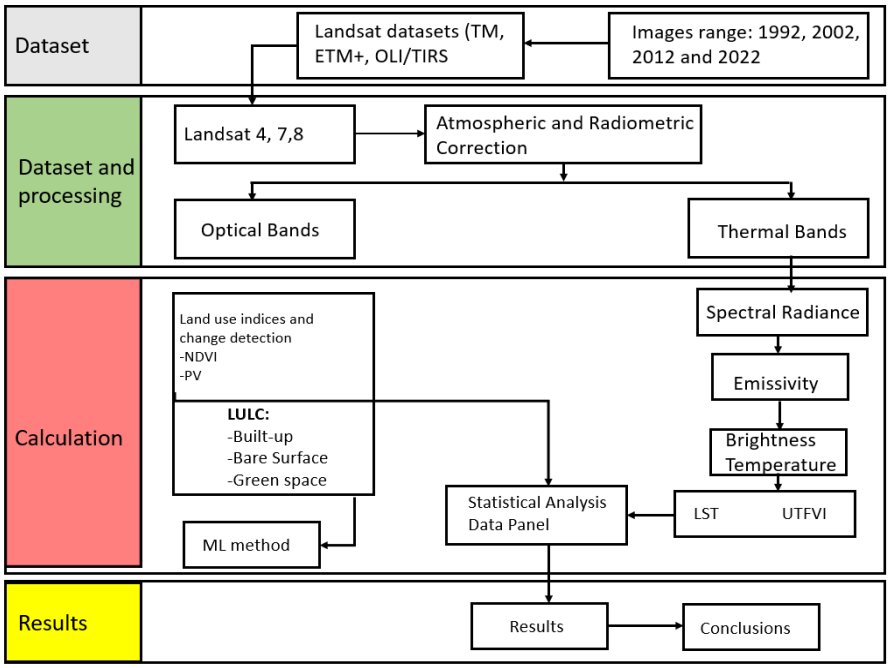

RESULT AND DISCUSSION

Land use/land cover dynamic in Phase One of the FCC (1992-2022)

Land use pertains to the specific human activities for which a particular piece of land is designated, encompassing categories such as commercial, industrial, and residential uses (Armson *et al.,* 2012). The alterations in land use have substantial implications for environmental sustainability at both local and regional scales (Weng, 2018). Certain land use changes lead to immediate shifts in land cover, exerting notable influences on surface temperature and climate, thereby possessing meteorological significance (Azarakhsh and Eduardo, 2016).

LULC Characterization in Phase One of FCC in 1992

In 1991, the three categories of land use land cover (Built-up area, bare surface, green space) distribution as presented in Figure 2 and Table 3 shows that green space constitute a significant portion of the area of extent 29.63km^2 (49.05%). The built-up area which is next covered 18.82 km2 (31.15%), bare surface occupied 11.96

km2 (19.80%).

LULC Characterization of Phase One of the FCC in 2002

The finding in the year 2002 reveals that amongst the three categories of the land use land cover (Built-up area, bare surface, green space) distribution as observed in Figure 4 and Table 3, green space had the largest space coverage of 24.50km^2 (40.56%) whereas built-up area spatial extent denoted 21.67km^2 (35.87%) and bare surface covered 14.23km^2 (23.55%) (Figure 3 and table 3).

LULC Characterization of Phase One of the FCC in 2012

The three categories of the land use land cover (Built-up area, bare surface, green space) distribution in the year 2012 as demonstrated in Figure 4 and Table 3 portrayed that built-up area had the largest space coverage of 28.42km^2 (47.05%) whereas bare surface spatial extent denoted 23.20km^2 (38.41%) and green space expressed an exponential decrease to 8.78km^2 (14.54%) due to rapid urbanization and human anthropogenic activities.

LULC Characterization of Phase One of the FCC in 2022

In 2022, the three categories of the land use land cover (Built-up area, bare surface, green space) distribution as presented in Figure 4.4 and Table 3 showed that built-up area had the principal extent of 38.35km^2 (63.50%) whereas bare surface spatial extent represented 14.77km^2 (24.46%) and green space depleted to 7.26km^2 (12.03%) (Figure 5 and table 3).

Table 3: Land use/land cover Characterization in Phase 1 of FCC in 1992

	Built-up area		**Bare surface**		**Green space**	
Year	Area (km)	%	Area (km)	%	Area (km)	%
1992	18.82	31.15	11.96	19.80	29.63	49.05
2002	21.67	35.87	14.23	23.55	24.50	40.56
2012	28.42	47.05	23.20	38.41	8.78	14.54
2022	38.35	63.50	14.77	24.46	7.26	12.03

Source: Researcher Analysis, 2024.

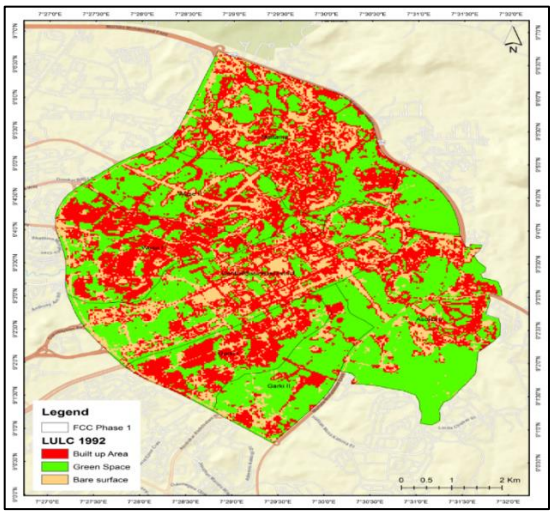

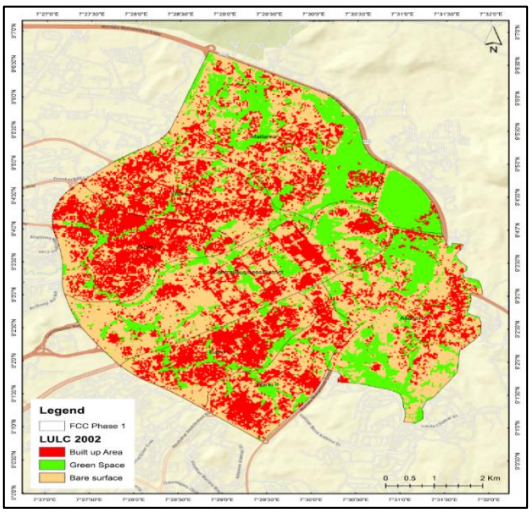

Figure 3: LULC Characterization in Phase 1 of FCC in 1992 Figure 4: LULC Characterization in Phase 1 of FCC in 2002

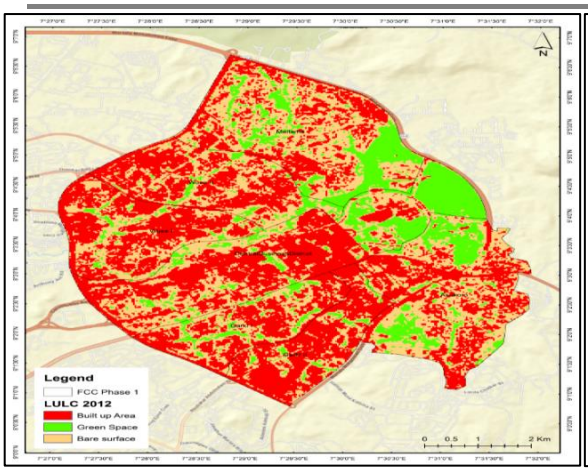

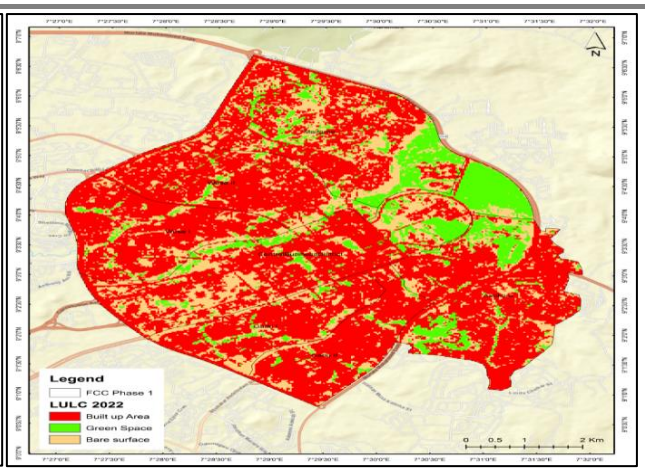

Figure 5: LULC Characterization in Phase 1 of FCC in 1992 Figure 6: LULC Characterization in Phase 1 of FCC in 1992

Land cover change matrix detection of Phase One of the FCC from 1992 to 2022

Table 4 and Figure 6 depict that from the year 1992 – 2022, the built-up area recorded a significant growth with +19.53km^2 (32.35%) with an annual rate change of 12.94% which is due to the rapid urbanization occurring in the study area. From the year 1992-2022, the bare surface experienced a spatial gain of +2.81 km^2 (4.66%) with an annual rate change of 1.86%. This is due to the transformation of the bare surface into construction sites for buildings. In Phase One of the FCC, vegetation recorded a decline of -22.37km^2 (-37.02%) with an annual change rate of -14.81% between the year 1992 to 2022 which is due to human anthropogenic activities occurring in that area for the period under study. The findings indicate a clear trend of swift land conversion within Phase One of the FCC, transitioning from bare surfaces and green spaces to built-up areas. This rapid transformation can be attributed to the high level of urbanization characterizing this particular region of the Federal Capital City. These findings are in agreement with the observations of Yuan-Bin, Yan-Hong and Lei (2021) in Fuzhou, China who examined the effects of changes in land use/cover on land surface temperature (LST). Zhaowu and Xieying (2018) observed a similar trend in their study of the variation in land surface temperature and cooling efficiency of urban green spaces Fuzhou China discovered that Rapid urbanization has caused significant land cover change (LCC). They found significant alterations in land use/cover types in the study area from 1993 to 2016, particularly notable changes in construction land arising from the agglomeration of five highly urbanized districts.

Figure 7: Land use/land cover transition matrix of Phase One of FCC (1992 -2022)

ISSN No. 2454-6186 | DOI: 10.47772/IJRISS |Volume VIII Issue XII December 2024

Table 4: Transition matrix of the land use/land cover of Phase One of the FCC (1992 – 2022)

Year	**1992 - 2002**		**2002 - 2012**		**2012 - 2022**		**1992 -2022**		**Annual rate**
Class	Area (km)	%	Area (km)	%	Area (km)	%	Area (km)	%	Inference
Built-up area	+2.85	4.72	+6.75	11.18	+9.93	16.45	+19.53	32.35	12.94
Bare surface	+2.27	3.75	+8.97	14.86	-8.43	-13.95	+2.81	4.66	1.864
Green space	-2.13	-8.49	-18.72	-26.02	-1.52	-2.5	-22.37	-37.02	-14.808

Source: Researcher analysis, 2024.

LST Characteristics and Decadal Changes in Phase One of the FCC from 1992 to 2022

Land Surface Temperature (LST) and urban growth are deeply intertwined, with each influencing the other in significant ways. The analysis of Land Surface Temperature (LST) from 1992 to 2022 reveals several trends and variations across different temperature ranges.

Table 5 depicts that the LST range of less than 22℃, increased in area from 2.07 km² to 3.65 km² between 1992 and 2002, reflecting a rise of 1.58 km². However, between 2002 and 2012, this area decreased from 3.65 km² to 2.76 km², a reduction of 0.89 km². The decreasing trend continued from 2012 to 2022, with the area further shrinking to 2.55 km², indicating a reduction of 0.21 km².

Area with LST range of 23.1℃ to 24℃ decreased significantly from 13.43 km² in 1992 to 9.58 km² in 2002, a loss of 3.85 km². This downward trend persisted into the next decade, with the area contracting from 9.58 km² in 2002 to 7.89 km² in 2012, a reduction of 1.69 km². However, from 2012 to 2022, the area rebounded, expanding from 7.89 km² to 10.03 km², an increase of 2.14 km². The trend of LST ranging from 23.1℃ to 24℃ increased in area coverage for the first and second decades but increased into the third decade of study (2012 to 2022) (See Table 5).

Area with LST range of 24.1℃ to 25℃ substantial increase from 7.65 km² in 1992 to 18.22 km² in 2002, a growth of 10.57 km². This upward trend continued between 2002 and 2012, with the area increasing from 18.22 km² to 19.28 km², an increase of 1.06 km². The area further expanded to 20.71 km² by 2022, marking an increase of 1.43 km² over the last decade. The trend of LST ranging from 24.1℃ to 25℃ consistently increase in area coverage from 1992 to 2022 (See Table 5).

It was observed that the area with LST of 25.1℃ to 26℃ decreased from 26.34 km² in 1992 to 19.03 km² in 2002, a reduction of 7.31 km². From 2002 to 2012, the area increased to 23.14 km², gaining 4.11 km². However, this was followed by a decline from 2012 to 2022, with the area reducing to 19.57 km², a decrease of 3.57 km². The trend of LST ranging from 25.1℃ to 26℃ wasn't consistent depicting a decrease, increase and decrease in area coverage from 1992 to 2022 (Table 5).

Within the study area, the LST of the area above 27℃ decreased from 10.99 km² in 1992 to 9.99 km² in 2002, a loss of 1.0 km². This decline continued between 2002 and 2012, with the area contracting to 7.41 km², a reduction of 2.58 km². From 2012 to 2022, there was a slight increase in area to 7.59 km², representing a modest rise of 0.18 km². Findings clearly show a decadal reduction in areas above 27℃ except for the last decade of study (2012 to 2022) (See Table 5).

In Phase One of the FCC area with a 24.1℃ – 25℃ increase in the area of 10.57 km² in 1992-2002, the area having 24.1℃ – 25℃ increase with 1.058 km² and an area of 25.1℃ – 26℃ increase with 4.111 km² from 2002 to 2012 while the area with above 27℃ increase with 0.179 km². These changes in area across different LST ranges over the three decades are attributed to urbanization changes in land use and land cover. The fluctuations indicate complex interactions between natural and anthropogenic factors influencing the land surface temperature dynamics of Phase One of the FCC. The findings slightly differ from the findings of

Yusuf, *et. al.,* (2023) who explored LST characterization and changes given swift urbanization in Nguru Local Government Area, Yobe State, Nigeria where they observed consistent rise in LST from 2001 to 2021. Also, Maurice, *et al.,* (2017) observed a relationship between LULC changes in the LST of Nairobi City but with a decadal variation.

Table 5: FCC Phase One Land Surface Temperature (LST in ºC)

LST (°C)	**1992 Area (km^2)**	**2002 Area (km^2)**	**Change Area (km^2)**	**2002 Area (km^2)**	**2012 Area (km^2)**	**Change Area (km^2)**	**2012 Area (km^2)**	**2022 Area (km^2)**	**Change Area (km^2)**
Less than 22	2.07	3.65	1.58	3.652	2.7589	-0.8931	2.7589	2.55	0.2089
23.1- 24	13.43	9.58	-3.85	9.58	7.891	-1.689	7.891	10.03	2.139
24.1 - 25	7.65	18.22	10.57	18.22	19.278	1.058	19.278	20.71	1.432
25.1 - 26	26.34	19.03	-7.31	19.03	23.141	4.111	23.141	19.57	-3.57
27 above	10.99	9.99	-1.0	9.99	7.411	-2.579	7.411	7.59	0.179
Total	**60.45**	**60.45**		**60.45**	**60.45**		**60.45**	**60.45**	

Source: Researcher analysis, 2024.

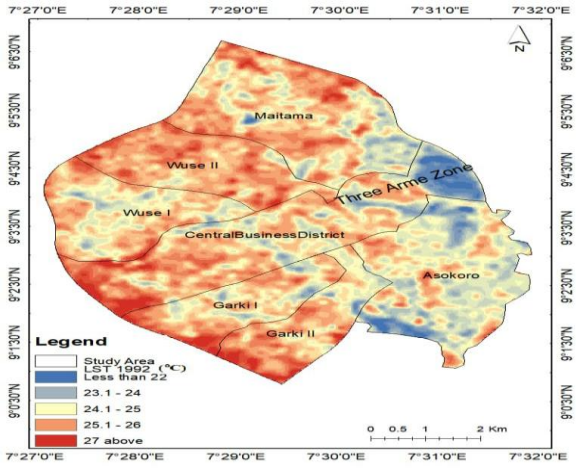

Figure 8: LST of Phase One of the FCC in 1992

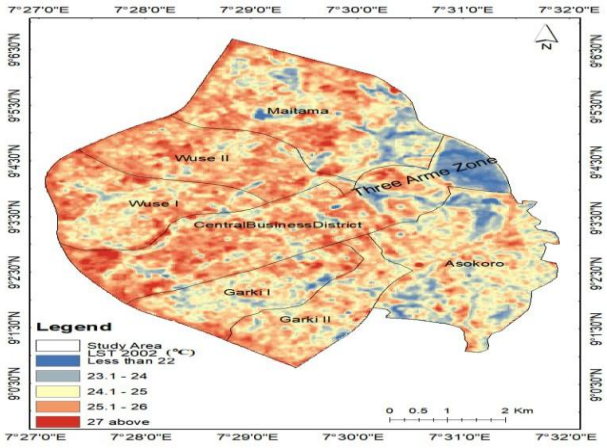

Figure 9: LST of Phase One of the FCC in 2002

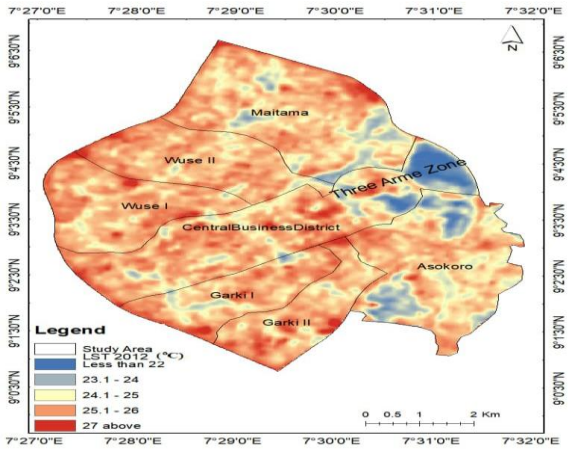

Figure 10: LST of Phase One of the FCC in 2012

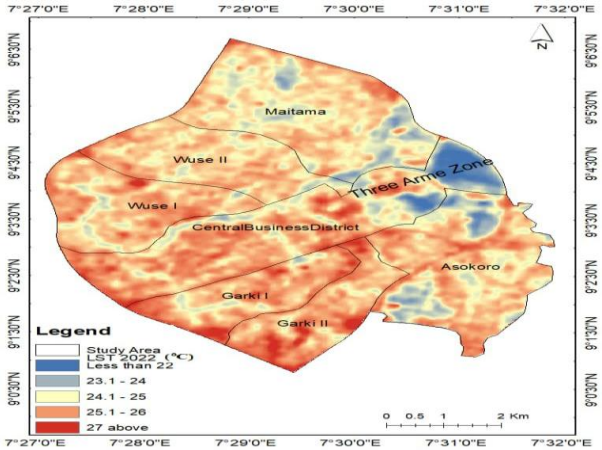

Figure 11: LST of Phase One of the FCC in 2022

ISSN No. 2454-6186 | DOI: 10.47772/IJRISS |Volume VIII Issue XII December 2024

Source: Researcher analysis, 2024.

Cooling efficiency of green spaces within Phase One of FCC from 1992 to 2022

In Phase One of the FCC in the Federal Capital Territory of Nigeria, cooling efficiency varied over the study period (1992-2022).

The cooling efficiency of green spaces within Phase One of FCC in 1992

In 1992, results indicate that 2.04km^2 in Phase One (mostly at the Three Arms Zone) had < 0 Ecological Evaluation Index (EEI) which means excellent cooling efficiency, area with good cooling efficiency covered (0.000–0.005 EEI) covered 11.63km^2 (19.23%) mostly in Asokoro area of the FCC, area with normal cooling efficiency (0.005–0.010 EEI) covered 5.54km^2 (9.17%) in the central part of the FCC, area with bad cooling efficiency (0.010–0.015 EEI) covered 19.25km^2 (31.43%) in Maitama, Wuse II, west of the CBD, west of Garki I and Garki II, central and southern part of the FCC. Area with worse cooling efficiency (>0.015 EEI) also dominates in Maitama, Wuse II, west of the CBD, west of Garki I and Garki II in Phase One of the FCC with an area coverage of 21.99km^2 (36.33%) of the FCC (See Table 4.8 and Figure 11).

Cooling efficiency of green spaces within Phase One of FCC in 2002

The cooling efficiency in Phase One of the FCC in the year 2002 indicates that area of 7.74km^2 (12.81%) of the FCC (the peak of the Three Arm Zone) had < 0 Ecological Evaluation Index (EEI) which means excellent cooling efficiency, area with good cooling efficiency (0.000–0.005EEI) covered 13.44km^2 (22.23%) is laced almost all part in the Phase One of FCC, It was observed that area with normal cooling efficiency (0.005–0.010 EEI) covered 5.91km^2 (9.78%) in almost all part of the FCC, an area with bad cooling efficiency (0.010–0.015 EEI) covered 17.28km^2 (28.59%) mostly at Maitama, Wuse II, and west of the CBD. Area with worse cooling efficiency (>0.015 EEI) also dominates mostly Maitama, Wuse I, Wuse II, and west of the CBD in Phase One of FCC with an area coverage of 16.08km^2 (26.60%) in Phase One of the FCC (See Table 4.8 and Figure 12).

Cooling efficiency of green spaces within Phase One of FCC in 2012

In the year 2012, Findings in Table 4.8 and Figure 13 area with < 0 Ecological Evaluation Index (EEI) which means excellent cooling efficiency covered 2.15km^2 (3.56%) in the Three Arms Zones of Phase One of the FCC, area with good cooling efficiency (0.000–0.005 EEI) covered 12.59km^2 (20.81%) mostly in Asokoro and Wuse I of Phase One of the FCC, an area with normal cooling efficiency (0.005–0.010 EEI) covered 6.73km^2 (11.15%) scattered in most of Phase One of the FCC except the Three Arm Zone, area with bad cooling efficiency (0.010–0.015 EEI) covered 18.83km^2 (31.17%) in Wuse I, CBD, Garki I and Garki II of Phase One of the FCC. Area with worse cooling efficiency (>0.015 EEI) also dominates Wuse I, CBD, Garki I and Garki II of Phase One of the FCC with an area coverage of 20.15km^2 (33.31%) (See Table 4.8 and Figure 13).

Cooling efficiency of green spaces within Phase One of FCC in 2022

The cooling efficiency in Phase One of the FCC in the year 2022 indicates that an area with < 0 Ecological Evaluation Index (EEI) which means excellent cooling efficiency covered 0.93km^2 (1.54%) of Phase One of the FCC (The Three Arms Zone), area with good cooling efficiency (0.000–0.005 EEI) covered 11.56km^2 (19.13%) found in slightly spread in almost all part in the Phase One of FCC. It was observed that the area with normal cooling efficiency (0.005–0.010 EEI) covered 7.46km^2 (12.33%) in almost all parts of Phase One of the FCC, area with bad cooling efficiency (0.010–0.015 EEI) covered 19.65km^2 (32.5%) mostly at Maitama, Wuse I, Wuse II, Garki I, Garki II and the CBD. Area with worse cooling efficiency (>0.015 EEI) also spread across Maitama, Wuse I, Wuse II, Garki I, Garki II and the CBD in Phase One of the FCC with an area coverage of 20.85km^2 (34.5%) in the Phase One of the FCC (See Table 4.8 and Figure 14).

Table 4.8: FCC Phase One of Ecological Evaluation Index (EEI)

EEI	**1992 EEI Distribution**		**2002 EEI Distribution**		**2012 EEI Distribution**		**2022 EEI Distribution**	
	km^2	**%**	**km^2**	**%**	**km^2**	**%**	**km^2**	**%**
< 0	2.04	3.38	7.74	12.81	2.15	3.56	0.93	1.54
0.000–0.005	11.63	19.23	13.44	22.23	12.59	20.81	11.56	19.13
0.005–0.010	5.54	9.17	5.91	9.78	6.73	11.15	7.46	12.33
0.010–0.015	19.25	31.43	17.28	28.59	18.83	31.17	19.65	32.5
>0.015	21.99	36.33	16.08	26.60	20.15	33.31	20.85	34.5
	60.45	**100**	**60.45**	**100**	**60.45**	**100**	**60.45**	**100**

Source: Researcher analysis, 2024.

Cooling Efficiency of Green Spaces Change Detection in Phase One of FCC from 1992 to 2022

The cooling efficiency of green space change detection explains the effectiveness of green spaces (like parks, gardens, or urban forests) in cooling urban environment changes over time. This is crucial because green spaces can significantly impact local temperatures and overall climate resilience.

Cooling Efficiency of Green Spaces Change Detection in Phase One of FCC from 1992 to 2002

In Phase One of FCC from 1992 to 2002, areas with excellent cooling efficiency (< 0) increased by 5.7km^2 (9.43%), areas with good cooling efficiency (0.000–0.005 EEI) increased by 1.81 km^2 (3%), areas with normal cooling efficiency (0.005–0.010 EEI) increased with an infinitesimal area of 0.37 km^2 (0.61%). There was a decrease in an area with bad cooling efficiency (0.010–0.015 EEI) with -1.97 km^2 (-2.84%). Also, an area with worse cooling efficiency reduces to -5.91 km2 (-2.84%) in Phase One of FCC from 1992 to 2002 (See Table 4.9). These findings show improved cooling efficiency in the Phase One of the FCC from 1992 to 2002.

Cooling Efficiency of Green Spaces Change Detection in Phase One of FCC from 2002 to 2012

From 2002 to 2012, an area with excellent cooling efficiency (< 0) decreased by -5.59km^2 (-9.25%), an area with good cooling efficiency (0.000–0.005 EEI) decreased by -0.85km^2 (-1.42%), an area with normal cooling efficiency (0.005–0.010 EEI) increased with an infinitesimal area of 0.82km^2 (1.37%). There was an increase in the area with bad cooling efficiency (0.010–0.015 EEI) of 1.55 km2 (2.58%). Also, an area with worse cooling efficiency increased by 4.07 km2 (6.71%) in Phase One of FCC from 2002 to 2012 (See Table 4.9). These findings show depreciating cooling efficiency in Phase One of the FCC from 2002 to 2012.

Cooling Efficiency of Green Spaces Change Detection in Phase One of FCC from 2012 to 2022

It was observed that from 2012 to 2022, areas with excellent cooling efficiency (< 0 EEI) decreased with -1.22km^2 (-2.02%), area with good cooling efficiency (0.000–0.005 EEI) decreased with -1.03km^2 (-1.68%), area with normal cooling efficiency (0.005–0.010 EEI) increased with minute area of 0.73km^2 (1.187%). There was also an increase in area with bad cooling efficiency (0.010–0.015 EEI) with 0.82 km2 (1.18%). Also, areas with worse cooling efficiency increased by 0.7 km2 (1.19%) in Phase One of FCC from 2012 to 2022 (See Table 4.9). These findings show depreciating cooling efficiency in Phase One of the FCC from 2012 to 2022.

The findings in this study manifest that cooling efficiency in Phase One of the FCC has been depreciating over

ISSN No. 2454-6186 | DOI: 10.47772/IJRISS |Volume VIII Issue XII December 2024

the past two decades. The consistent loss of green spaces to built-up areas which includes expansion of roads, introduction of new buildings and pavement development reduces the amount of land available for green spaces, leading to a decrease in cooling effects which is a function of the systematic rise in LST in Phase One of the FCC from 1992 to 2022.

Azarakhsh and Eduardo (2016) affirm that the conversion of parks and open areas into commercial or residential developments directly reduces the cooling capacity of these spaces. Isioye and, Ikwueze (2020) observed that poor maintenance can lead to overgrown or unhealthy vegetation thereby reducing its cooling impact. High levels of air pollutants can impair plant growth and function, reducing the effectiveness of green spaces in cooling the environment and accumulation of particulate matter on vegetation can affect its transpiration rates and overall health as observed by Emechebe and Eze (2019); Rahman *et al.,* (2020). Over the past two decades, the green spaces in Phase One of the FCC could only be seen in isolated patches and disconnected green spaces are less effective at cooling than larger, continuous areas. Fragmentation of green spaces reduces the overall cooling potential of urban green infrastructure. This was also observed by Park, et al., 2017 and Li et al., 2019.

Table 4.9: Changes in FCC Phase One Ecological Evaluation Index (EEI)

EEI	**1992-2002 Change**		**2002-2012 Changes**		**2002-2012 Changes**	
	km²	**%**	**km²**	**%**	**km²**	**%**
< 0	5.7	9.43	-5.59	-9.25	-1.22	-2.02
0.000–0.005	1.81	3	-0.85	-1.42	-1.03	-1.68
0.005–0.010	0.37	0.61	0.82	1.37	0.73	1.18
0.010–0.015	-1.97	-2.84	1.55	2.58	0.82	1.33
>0.015	-5.91	-9.73	4.07	6.71	0.7	1.19

Source: Researcher analysis, 2024.

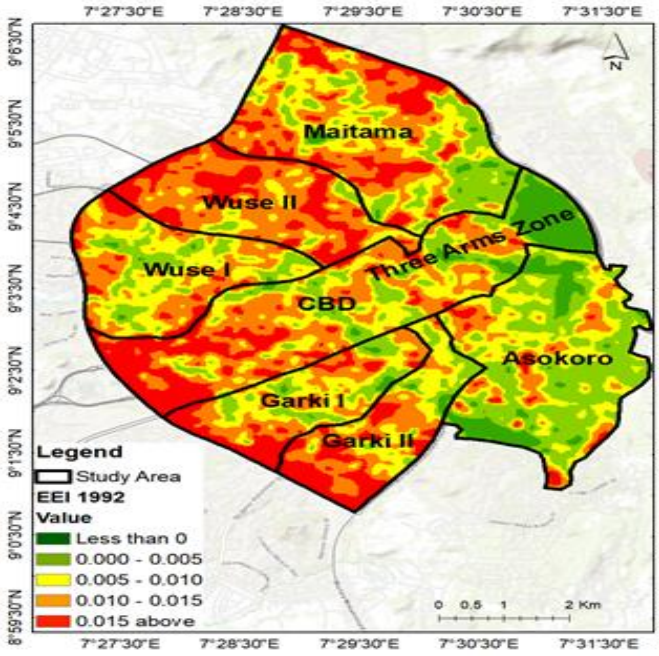

Figure 12: EE of Phase One of the FCC in 1992

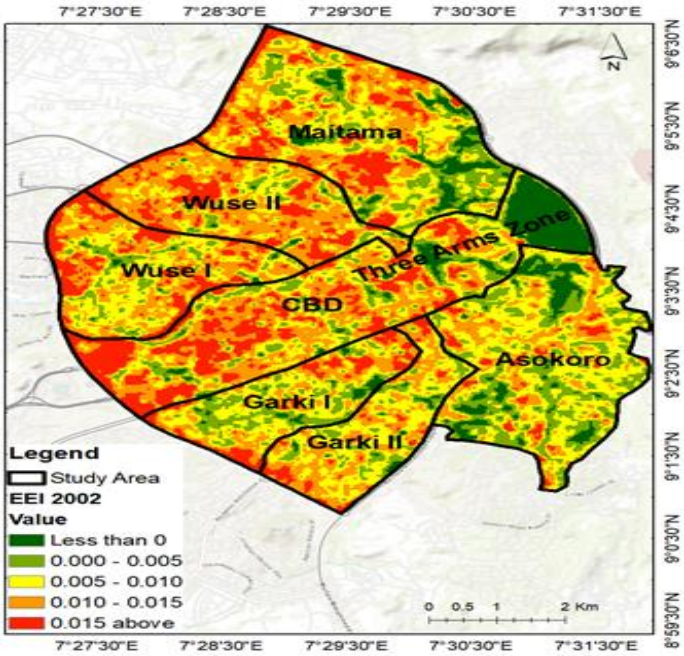

Figure 13: EE of Phase One of the FCC in 2002

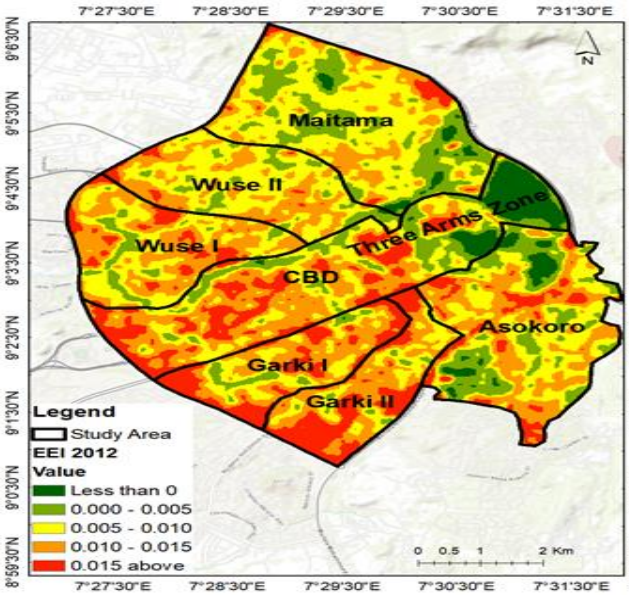

Figure 14: EE of Phase One of the FCC in 2012

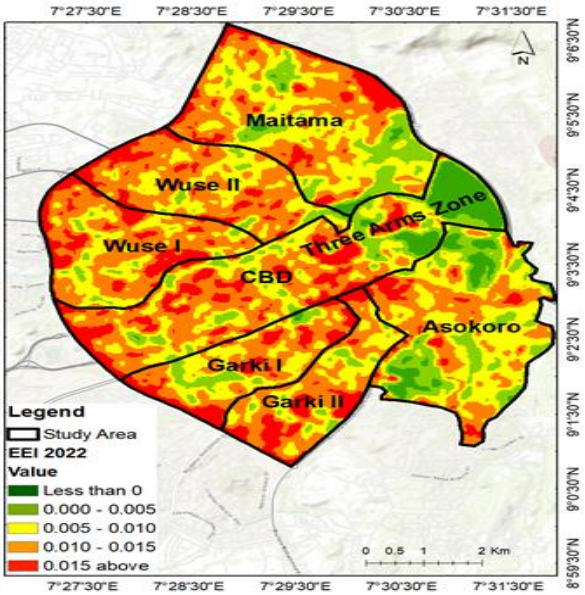

Figure 15: EE of Phase One of the FCC in 2022

Source: Researcher analysis, 2024.

CONCLUSION AND RECOMMENDATIONS

This study systematically analyzed the changes in land use, land cover, and the spatial variation of land surface temperature (LST) over three decades. Additionally, the cooling efficiency of green spaces was evaluated using the Ecological Evaluation Index (UTFVI). The temporal assessment revealed an increasing trend in both built-up areas and LST in the Federal Capital City (FCC), primarily concentrated in the northwest. The study concluded that not only an expansion of land surface temperature but also a decrease in the cooling efficiency of green spaces, attributed to vegetation loss and increased urbanization. Furthermore, the intensity of UTFVI significantly surged between 1992 and 2022, posing a threat to the cooling efficiency of green spaces in Phase One of the FCC. Based on the findings of this study, the following recommendations were made;

i. Enhanced Green Space Management in the FCC: This could be by **i**ncreasing the number and size of green spaces by developing new parks, gardens, and green corridors to enhance cooling effects. In achieving this planting of variety of species that are native or well-adapted to local conditions and ensuring regular maintenance of existing green spaces to keep vegetation healthy and maximize their cooling potential

ii. Innovative of Green Infrastructure in the FCC: The introduction of green roofs and walls on buildings can significantly reduce heat absorption and improve cooling efficiency.

iii. Development of Urban Forestry in the FCC**:** Implement urban forestry programs to increase tree canopy coverage can provide significant shade and cool the air through evapotranspiration.

iv. Encouraging Permeable Surfaces in the FCC: Use permeable pavements and surfaces to reduce heat retention and allow for better water infiltration.

REFERENCES

1. Adakayi, P.E; Ishaya S. (2016). Annual Trend of Minimum Temperature in Some Parts of Northern Nigeria. Ethiopian Journal of Environmental Studies and Management. 9(2): 220-227.
2. Armson, D., Stringer, P., & Ennos, A. R. (2012). The effect of tree shade and grass on surface and globe temperatures in an urban area. Urban Forestry & Urban Greening, 11(3), 245-255.
3. Arnberger, A., Eder, R., Allex, B., & Sterl, P. (2012). Visitors' attitudes towards remnant beech forest and visitor management preferences in two different situations. Urban Forestry & Urban Greening,

11(2), 169-177.
4. Azarakhsh R., Eduardo D. (2016). Local impact of tree volume on nocturnal urban heat island: A case study in Amsterdam. Department of Spatial Economics/SPINlab, VU University Amsterdam, De Boelelaan 1105, 1081 HV Amsterdam. http://dx.doi.org/10.1016/j.ufug.2016.01.008
5. Balogun O (2001). The Federal Capital Territory of Nigeria: A Geography of its Development. University Press, Ibadan
6. Balzarini, M. G., Paoletti, E., & Van Dingenen, R. (2009). Evaluation of the potential effectiveness of urban green areas as passive air quality control measures. Urban Forestry & Urban Greening, 8(2), 129-140.
7. Caiyan Y.B.; Li K.; Chen, Y.H.; Wu L.; Pan W.B. (2021) The Changes of Heat Contribution Index in Urban Thermal Environment: A Case Study in Fuzhou. Sustainability,, 13, 9638. https://doi.org/10.3390/ su13179638
8. Chen, X., Zhao, H., Li, W., Yin, L., & Yin, Z. (2011). Rapid urbanization in China: A real challenge to soil protection and food security. CATENA, 85(2), 75-81.
9. Emechebe, L.C., & Eze, C.J. (2019). Integrating Sustainable Urban Green Space as a Means to Reduce Intense Heat in Residential Areas: A Case Study of Abuja, Nigeria. Environmental Technology & Science Journal. 10 (2), 24-32.
10. Hassan S.M. and Ishaya S**.** (2010). Vulnerability of Federal Capital Territory of Nigeria (Abuja) to Climate Change. Confluence Journal of Environmental Studies. 5:10-19.
11. Ishaya, S. (2020). Assessment of Urban Generated Climate Anomaly in Okene Town, Okene Local Government Area of Kogi State, Nigeria. FUDMA Journal of Sciences (FJS)**.** 4(2): 101-110. DOI: https://doi.org/10.33003/fjs-2020-0402-203
12. Isioye O. and, Ikwueze (2020) Urban heat island effects and thermal comfort in Abuja Municipal area council of Nigeria.Department of Geomatics, Ahmadu Bello University, Zaria Nigeria. FUTY Journal of the Environment. 14(2), 13-24.
13. Li, D., Bou-Zeid, E., & Oppenheimer, M. (2019). The effectiveness of cool and green roofs as urban heat island mitigation strategies. Environmental Research Letters, 14(4), 044022.
14. Lindsey, G., Maraj, M., & Kaza, N. (2017). Community development in green infrastructure: A case study of urban community gardens in Washington, DC. Community Development, 48(2), 290-305.
15. Maurice O., Faith N., Victor A. (2017). Modelling the Effect of Land Use and Land Cover Variations on the Surface Temperature Values of Nairobi City, Kenya. School of the Built Environment, Department of Architecture and Building Science, University of Nairobi, Nairobi, Kenya. Resources and Environment. 7(6): 145-159 DOI: 10.5923/j.re.20170706.01
16. Oke, T. R. (2017). The Micrometeorology of the Urban Forest. Philosophical Transactions of the Royal Society B: Biological Sciences, 324(1223), 335-349.
17. Olubukola C. O., Ishaya S, Esemuze., Adakayi P. E (2023). Spatio-Temporal Occurrence of Climate Change: Evidence from Rainfall and Temperature Records in the Agro-Ecological Zones of Ondo State, Nigeria. World Scientific News 182: 237-249.
18. Parka Jonghoon, Jun-Hyun Kima, Dong Kun Lee b, Chae Yeon Park b, Seung Gyu Jeong (2017). The influence of small green space type and structure at the street level on urban heat island mitigation. Urban For. Urban Green. 3(2), 21-32.
19. Rahman, Mohammad A. Laura Stratópoulos., Astrid Moser-Reischl., Stephan Pauleit (2019). Traits of trees for cooling urban heat islands: A meta-analysis. Building and Environment. 170(7):106606
20. Sadroddin, A., Martin W., and Salman Q. (2014), The Role of Vegetation in Mitigating Urban Land Surface Temperatures: A Case Study of Munich, Germany during the Warm Season. Sustainability, 7(4), 4689-4706; https://doi.org/10.3390/su7044689
21. Tan, P. Y., & Jim, C. Y. (2013). Urban green spaces in high-density cities: A case study of Hong Kong and Singapore. Ecological Indicators, 34, 97-106.
22. Tangban E. E., Oku E. E., Ishaya S. and Boscolo R (2020). Quantification and delineation of aridity boundaries in Northern Nigeria. Journal of Agriculture and Ecosystem Management. 1(1) 21-
23. Van den Bosch & Ode Sang, (2017). Urban natural environments as nature-based solutions for improved public health: A systematic review of reviews. Environmental Research 158:373-384
24. Weng, Q. (2018). Advances in urban remote sensing: Overview and reflections. Remote Sensing of Environment, 219, 1-3.

25. Wong, N. H., Chen, Y., Ong, C. L., & Sia, A. (2017). Greenery and thermal comfort of the urban microclimate in a tropical city. Built Environment, 43(2), 188-203.
26. Wong, N. H., Tan, C. L., Kolokotsa, D., & Takebayashi, H. (2021). Greenery as a mitigation and adaptation strategy to urban heat. Nature Reviews Earth & Environment, 2(3), 166-181
27. Yan, L.; Jia, W.; Zhao, S. (2021) The Cooling Effect of Urban Green Spaces in Metacities: A Case Study of Beijing, China's Capital. Remote Sens. 13(22), 4601; https://doi.org/10.3390/rs13224601
28. Yusuf, Y. Y., Hassan G. M., Mohammed D., Usman A. M., Umar M A., Abdullahi A. A (2023). Analysis of Two Decades Variations in Urban Heat Island Using Remotely Sensed Data in Nguru Local Government Area, Yobe State, Nigeria, International Journal of Environment and Geoinformatics (IJEGEO), 10(2): 110-119. doi.10.30897/ijegeo.1220431
29. Zhaowu Y., Xieying G., Yuxi Z., Motoya K., Henrik V.(2018).Variations in land surface temperature and cooling efficiency of green space in rapid urbanization: The case of Fuzhou city, China. Geography Science and Resource Institute, Chinese Academy of Sciences, Beijing, 100101, China https://doi.org/10.1016/j.ufug.2017.11.008